BBA - Molecular Cell Research xxx (xxxx) xxxx

Contents lists available at ScienceDirect

BBA - Molecular Cell Research

journal homepage: www.elsevier.com/locate/bbamcr

A dynamic link between H/ACA snoRNP components and cytoplasmic stress granules

Valentina Belli[1], Nunzia Matrone[1], Serena Sagliocchi, Rosa Incarnato, Andrea Conte, Elio Pizzo, Mimmo Turano, Alberto Angrisani*, Maria Furia*

Department of Biology, University of Naples "Federico II", Complesso Universitario Monte Santangelo, via Cinthia, 80126 Napoli, Italy

ARTICLE INFO

Keywords:
Dyskerin
snoRNPs
RNP bodies
Ribosome
Nucleolus
Stress response

ABSTRACT

Many cell stressors block protein translation, inducing formation of cytoplasmic aggregates. These aggregates, named stress granules (SGs), are composed by translationally stalled ribonucleoproteins and their assembly strongly contributes to cell survival. Composition and dynamics of SGs are thus important starting points for identifying critical factors of the stress response. In the present study we link components of the H/ACA snoRNP complexes, highly concentrated in the nucleoli and the Cajal bodies, to SG composition. H/ACA snoRNPs are composed by a core of four highly conserved proteins -dyskerin, Nhp2, Nop10 and Gar1- and are involved in several fundamental processes, including ribosome biogenesis, RNA pseudouridylation, stabilization of small nucleolar RNAs and telomere maintenance. By taking advantage of cells overexpressing a dyskerin splice variant undergoing a dynamic intracellular trafficking, we were able to show that H/ACA snoRNP components can participate in SG formation, this way contributing to the stress response and perhaps transducing signals from the nucleus to the cytoplasm. Collectively, our results show for the first time that H/ACA snoRNP proteins can have additional non-nuclear functions, either independently or interacting with each other, thus further strengthening the close relationship linking nucleolus to SG composition.

1. Introduction

One of the mechanisms by which cells cope with various types of stress is the formation of ribonucleoprotein cytoplasmic foci, named stress granules (SGs), whose aggregation helps cells to acquire adaptation to stress conditions and promote survival [1]. Stressed cells limit translation initiation, causing disassembly of polysomes and stalling of initiation complexes which are then recruited in SGs [2,3]. Typical SG markers are thus various translation initiation factors (eIF3, eIF4A eIF4E and eIF4G), 40S ribosomal subunits and many RNA binding proteins, most commonly TIA1 (T-cell internal antigen 1), G3BP1 (Ras-GTPase-activating protein SH3-domain binding protein 1) and PABP (PolyA-binding protein). Several recent reports indicated that SGs have a shell-like structure, in which a stable "core", composed by highly concentrated nucleating factors, is surrounded by a less dense but strictly interconnected "shell" whose composition is more dynamic [4,5]. Liquid-liquid phase separation (LLPS) is thought to be the general mechanism driving the formation of membrane-less foci, including SGs [6,7] and several observations suggest that intrinsically disordered regions (IDRs) on RNA-binding proteins have a relevant role in their assembly, favoring LLPS [8,9]. Being SGs non-membranaceus bodies, RNAs and proteins are free to shuttle in-out, in a dynamic equilibrium with polysomal mRNAs and other cytoplasmic RNA granules, such as P- and GW182-bodies. P-bodies, that are present also in non-stressed cells, are linked to translation inhibition and RNA decay; they accumulate decapping and deadenylation factors, and their number increases upon stress [10]. Although often associated with P-bodies, GW182 bodies [11–13] represent a distinct pool of granules involved in microRNA-mediated translational silencing that are specifically identified by presence of the GW182 protein [14]. All these types of cytoplasmic RNA granules are unstable and exhibit dynamic interactions, such as docking or fusion, exchanging components and possibly evolve from one type to another [13,15]. This complex trafficking, together with intrinsic features of mRNAs (such as presence of ARE elements) and posttranslational modifications of mRNA binding proteins, all concur in selecting the fate of cytoplasmic mRNAs, addressing these molecules to either silencing, storage, or decay [16,17]. The cytoplasmic RNP granules share many similarities with nucleoli, whose organization is thought

* Corresponding author at: Department of Biology, University of Naples, via Cinthia, 80126 Napoli, Italy.
E-mail addresses: alberto.angrisani@unina.it (A. Angrisani), mfuria@unina.it (M. Furia).
[1] Present address: Department of Precision Medicine, Università degli studi della Campania "Luigi Vanvitelli", Napoli, Italy.

https://doi.org/10.1016/j.bbamcr.2019.118529
Received 17 January 2019; Received in revised form 8 July 2019; Accepted 5 August 2019

equally be regulated by LLPS. Nucleoli are known to play a key role in coordinating stress response and, upon stress exposure, many nucleolar proteins are recruited in SGs [18]. In this report, we identify nucleolar dyskerin and other core components of the H/ACA small nucleolar ribonucleoprotein (snoRNPs) as novel components of SGs, further reinforcing this connection. Dyskerin is a highly conserved multifunctional protein that acts as RNA-guided pseudouridine synthase, directing the enzymatic conversion of specific uridines to pseudouridines. It concentrates in the nucleoli and the Cajal bodies (CBs) where, in association with three other highly conserved proteins -Nop10, Nhp2, Gar1- composes a tetramer able to enter in the composition of different nuclear RNPs playing key biological functions [19]. Within the nucleolus, the tetramer associates with H/ACA small nucleolar RNAs (snoRNAs) to compose the H/ACA snoRNPs, that regulate rRNA processing and pseudouridylate RNA targets by snoRNA-guided base complementarity [20,21]. Within the CBs, it associates with CB specific small RNAs (scaRNAs) to compose the scaRNPs, that direct pseudouridylation of spliceosomal snRNAs [22]. Finally, in association with the human telomerase RNA (TERC), the tetramer enters in the formation of the active telomerase complex that regulates telomere maintenance [23]. In addition to these well-established functions, dyskerin has been involved in a variety of disparate biological processes, including regulation of IRES-dependent translation [24] and antioxidant/DNA damage response [25–28]. Several data from the Drosophila *in vivo* animal model highlighted that dyskerin is deeply implicated in the regulation of cell homeostasis [29–31]. In humans, the impact of dyskerin is further outlined by the fact that its loss-of-function causes the X-linked dyskeratosis congenita disease [32] and its severe variant Hoyeraal-Hreidarsson syndrome [33], while its overexpression characterizes several types of aggressive cancers [34–42].

Considering the significant interest in deciphering the variety of dyskerin functions, we analyzed in detail the expression dynamics of a truncated dyskerin splice isoform, named isoform 3 (thereafter called Iso3), that shows an unexpected cytoplasmic localization [43]. Recently, this isoform attracted further interest for its recent involvement in either lipid [44] and mitochondrial metabolism [45]. We show here that this dyskerin variant can have a dual nucleo-cytoplasmic localization, compatible with a role in transducing signals connecting nucleus and cytoplasm. Together with the full-length major dyskerin isoform and the other H/ACA snoRNP core components, this protein can be recruited to SGs, thus revealing that H/ACA snoRNP components can have non-nucleolar functions that can contribute to cellular stress response, this way promoting cell survival.

2. Materials and methods

2.1. Cell culture and treatments

HeLa cells used in this study were stably transfected with the p3XFLAG-CMV-10 vector expressing the FLAG-tagged Isoform 3 (3XF-Iso3) or with the p3XFLAG-CMV-10 vector without insert (control cells; 3XF-Mock) as previously described [43]. Cells were cultured in high glucose DMEM (ECB7501L) supplemented with 10% fetal bovine serum (ECS0120DI), Penicillin (100.0 U/mL)/Streptomicin (100.0 mg/mL) (ECB3001D), L-Glutamine 200.0 mM (ECB3000D, all from EuroClone, Milan, Italy), grown at 37 °C in a humidified atmosphere and selected with G418 0.5 mg/mL (G418-RO, F. Hoffmann–La Roche SA, Basel, Switzerland). Before each treatment, cells were washed with PBS, resuspended in fresh DMEM containing the selected drug and incubated at 37 °C in a humidified atmosphere with 5% CO_2 for the selected time. For sodium arsenite treatment (S7400, Sigma-Aldrich, St. Louis, USA) cells were exposed for 1 h to 250 μM pH 6 $NaAsO_2$; for cycloheximide treatment, cells were incubated in 10 μg/mL cycloheximide (02194527, MP Biomedicals, Santa Ana, USA) for 30 min; for malonate treatment (136,441, Sigma) cells were incubated 12 h in 100 mM malonate; for etoposide treatment (E1383, Sigma) cells were incubated 1 h in 50 μM etoposide; for proteasome inhibition treatment cells were exposed for 1 h to 5.0 μM each of a mix of *inhibitor I, Lactacystin, MG132* (539,164, Set I – Calbiochem Darmstadt, Germany). Following each treatment, cells were analyzed by Immunofluorescence or Western Blotting as described below.

2.2. Immunofluorescence analysis

Cells were cultured overnight on coverslips, washed with PBS, fixed with 4% paraformaldehyde (158127, Sigma) for 10 min, permeabilized with 0.3% Triton X-100 (41,810, NorgenBiotek, Ontario, Canada) in PBS for 15 min and blocked with 3% BSA (1183GR100, neoFroxx, Einhausen, Germany) in PBS for 30 min at room temperature. After washing, cells were incubated with primary antibodies for 2 h at room temperature and then with secondary antibodies for 1 h at room temperature. Immunofluorescence micrographs were taken by Zeiss LSM 700 microscope (Zeiss, Oberkochen, Germany) using EC Plan-Neofluar 40× or Plan-Apochromat 63×/1.40 Oil immersion objectives, or by Leica TCS-SP5 MP (Leica, Solms, Germany) using HC PL IRAPO 40× or 63× water objectives. Images were analyzed by ImageJ (http://imagej.nih.govt/ij/) or Zeiss Zen software tools. Antibodies used are listed in Appendix A, Table S1.

2.3. Protein extraction and western blot analysis

Cells were washed with ice-cold PBS, collected and centrifuged at 1400 rpm for 5 min. Pellets were resuspended in a lysis buffer containing 50 mM Tris pH 8.0 (1115KG001, neoFroxx), 150 mM NaCl, 5 mM EDTA (1073, J.T.Baker, Radnor, USA), 1% NP40 (A1694,0250, AppliChem Darmstadt, Germany), supplemented with Complete inhibitor cocktail (11,836,153,001, Roche), incubated in ice and mechanically mixed by vortexing. Supernatants were collected after centrifugation at 14000 rpm for 15 min at 4 °C. The protein concentration was measured using the Bio-Rad protein assay (#5000006, Bio-Rad, Hercules, USA) following manufacturer instructions. Cell lysates were separated by SDS/PAGE in 10 or 15% gels using Sharpmass VI Plus (EPS025500, EuroClone) as protein ladder. Separated proteins were blotted onto nitrocellulose membrane (10,600,002, GE Healtcare, Chicago, USA). Membranes were blocked with 10% fat free milk (1172GR500, neoFroxx) in TBS for 1 h and incubated with the appropriate antibodies listed in Table S1. Bands were visualized by ECL (#1705061, Bio-Rad) using the ChemiDoc XRS+ System (Bio-Rad), quantified with Image Lab Software (Bio-Rad) and analyzed by Excel software (Microsoft, Redmond, USA).

3. Results

3.1. Dyskerin Iso3 is partitioned between the nucleus and the cytoplasm and is efficiently recruited at sites of nuclear H/ACA snoRNPs assembly

Canonical full-length dyskerin (Isoform1) carries three highly evolutionarily conserved functional regions: the dyskerin-like domain (DKLD), the TruB_N pseudouridine synthase catalytic domain and the PUA-RNA binding domain; in addition, two Nuclear Localization Signals (NLS), localized respectively at the N- and C– ends, restrict this protein mainly inside the nucleus, where it concentrates in nucleoli and CBs (see Fig. 1A top left). The truncated dyskerin isoform 3, that retains all functional domains but lacks the C-terminal bipartite NLS, exhibits instead a prevalent cytoplasmic localization [43]. To investigate in more detail the Iso3 expression pattern, we performed by immunofluorescence confocal microscopy (IF) a large-scale analysis of previously obtained stably transfected cells overexpressing the Flag-tagged protein (3XF-Iso3 cells) [43]. This approach revealed that expression of the protein was characterized by highly variable levels, with a few of cells accumulating the protein at a significantly higher-than average extent (High-Level-Producing HLPs) in respect to the majority (Low-

level Producing, LLPs; see Fig. 1A, right; Appendix A, Fig. S1A). This variability was constantly reproduced in independently isolated stable clones and could not be eliminated by repeated clonal selection (Fig. S1A). Fluctuating levels have been described also for canonical dyskerin [46], and in some cases correlated with telomere length [47]. In our analyses, we also noted that cytoplasmic aggregates could occasionally be visualized in 3XF-Iso3 cells (Fig. 1A, bottom left); moreover, the Flag-tagged protein showed a highly variegated localization, with same cells expressing the protein only in the cytoplasm, some only in the nuclei, and others in both compartments (Fig. 1A right), thus suggesting the possibility that it could be dynamically subdivided between the cytoplasm and the nucleus. Within the nucleus, the protein concentrates into specific domains: to define them we co-immunostained cells with antibodies against fibrillarin and the endogenous full-length dyskerin (isoform 1; marked with a widely used antibody recognizing the C-terminal region, mostly deleted in Iso3 sequence [43]). Colocalization of Flag signal with either fibrillarin (Fig. 1B) and dyskerin (Fig. 1C) indicated that Iso3 concentrates in nucleoli and CBs, the two intimately linked subnuclear territories where these two proteins typically reside. Hence, the missing C-terminal NLS proved to be unnecessary not only for nuclear, but even for nucleolar dyskerin localization. It is worth noting that Iso3 concentrates mainly in the internal nucleolar fibrillar center, where rRNA transcription and early steps of snoRNP assembly occur, and in the dense fibrillar component, where rRNA processing takes place and nascent snoRNPs accumulate; in some cells this isoform even displaces endogenous canonical dyskerin from inner nucleolus regions, with this latter remaining concentrated in the dense fibrillar component and the CBs (Fig. 1C). This suggests that Iso3 can successfully compete with canonical dyskerin in the composition of snoRNPs, being even preferentially recruited at early phases of rRNA production and snoRNP assembly. To check whether it could efficiently be engaged also in mature H/ACA snoRNPs, we looked at its colocalization with Gar1, which is known to replace NAF1 at late H/ACA snoRNPs assembly stages [48]. Gar1 lacks a canonical NLS and can diffuse both in nucleoplasm and cytoplasm under either physiological or stress conditions [28]; its specific localization pattern is presumed to be modulated by protein-protein interaction and/or metabolic conditions. In our experiments we confirmed the Gar1 composite staining pattern and found that this protein colocalized with Iso3 in both cytoplasm and nucleus. Within the nucleus, Gar1 and Iso3 colocalized mainly at the CBs, where the exchange between NAF1 and Gar1 is thought to occur [48], but also at the nucleolar dense fibrillar/granular component (Fig. 1D). Thus, IF data collectively support the conclusion that Iso3 can participate in the formation of both nascent and mature H/ACA snoRNPs. It is worth noting that the recruitment of different dyskerin isoforms might confer diverse specificities to these modification complexes and thus have functional relevance, especially considering that specific pseudouridylation events, or a fraction of the modified residues, are specifically regulated and can depend on stress, tissue, or growth basis [49–51].

3.2. Expression of dyskerin Iso3 is highly variable and tightly regulated by proteasomal-dependent degradation

Since expression of the Flag-tagged Iso3 originates from a coding construct controlled by CMV promoter and lacking both 5′ and 3’ UTRs [43], we supposed that its variable level could mainly be decay-dependent. To assess this point, we exposed 3XF-Iso3 cells for variable times to cycloheximide (CHX), which inhibits protein biosynthesis by preventing translational elongation, and then examined protein extracts by western blotting analysis. CHX treatment caused an immediate drop of Iso3 level to became markedly reduced after 4 h; in the same conditions, canonical dyskerin was instead more stable (Fig. 2A; Appendix A, Supplemental Fig. S2A). Since several sites of protein modifications, such as SUMOylation and phosphorylation, lie in the dyskerin C-terminal region that is missing in the Iso3 truncated sequence [19,52], it is plausible that their presence contributes to extend dyskerin half-life. Alternatively, it is conceivable that a prompt aggregation with other snoRNP components, or the formation of specific complexes, may better protect full-length dyskerin from degradation. To gain more information about the degradative pathways to which Iso3 could specifically be addressed, we looked at two key proteolytic branches: the lysosomal-autophagic route and the ubiquitin–proteasome system. First, we analyzed by confocal microscopy the expression of two key autophagy regulators: Lamp2, that regulates the autophagosome-lysosome fusion and marks the lysosome membrane, and LC3, that regulates autophagosome biogenesis [53]. No significant Iso3-Lamp2 colocalization, or expansion of the lysosome compartment was observed even in 3XF-Iso3 highly overexpressing cells (HLPs), indicating that lysosome biogenesis was not stimulated (Fig. 2B). However, Lamp2-Flag signals occasionally overlapped in the nucleoli (Fig. 2B, inset). Although the biological significance of this finding remains to be established, a sporadic nuclear localization of Lamp2 is in good agreement with the composition of its physical interactome (available at https://thebiogrid.org), which in fact includes several nuclear, and also nucleolar, proteins. In keeping with the Lamp2 pattern, *LC3*-specific *punctuate* dots corresponding to autophagosomes were not detected in 3XF-Iso3 cells where, as expected for non-autophagic cells, LC3 signal marked the nucleus [54] and diffused uniformly in the cytoplasm (Fig. 2C). To check whether the efficiency of autophagic process was fully preserved, we next treated 3XF-Iso3 and control cells carrying the 3XFlag empty vector (hereafter called 3XF-Mock) with sodium arsenite, which induces oxidative stress and triggers both autophagy and SG aggregation [55]. Western blot analyses showed that the LC3-phosphatidylethanolamine conjugated form (LC3-II), known to be recruited to autophagosomal membranes, was efficiently induced in both cell lines; moreover, p62, a substrate widely used to mark the efficiency of the process [56], did not increase respect to 3XF-Mock cells upon autophagy stimulation, attesting the regularity of the autophagic flux (Fig. 2D, left). Intriguingly, IF analyses not only confirmed that LC3 autophagic puncta were efficiently induced in 3XF-Iso3 cells but revealed that upon arsenite treatment Iso3 protein aggregates in cytoplasmic foci strictly resembling SGs (Fig. 2D, right). This finding attracted our attention, pushing us to investigate more deeply this aspect (see next paragraph). Having established that Iso3 overexpression *per se* did not induce autophagy, nor the protein was addressed to lysosome-mediated degradation, we looked at the ubiquitin–proteasome system that is responsible for about 90% of extra-lysosomial protein degradation and plays a key role in the degradation of short-lived, misfolded or damaged proteins. Then, we prevented proteasomal activity by a combination of *proteasome inhibitor I, Lactacystin, MG132 and found that* Iso3 accumulation showed a marked increase, while the level of endogenous canonical dyskerin raised more modestly (Fig. 2E; Appendix A, Supplemental Fig. S2B). Collectively, these results indicated that Iso3 expression is tightly regulated at the post-transcriptional level by proteasome-mediated degradation. Considering the roles recently attributed to this isoform [44,45], it is plausible that its levels could dynamically be adapted to cell metabolic conditions.

3.3. Iso3 overexpression per se does not induce oxidative stress, unfolded protein response, or DNA damage

Having observed that arsenite treatment triggers Iso3 aggregation into cytoplasmic foci strictly resembling SGs (Fig. 2D, right), we wished to check whether overexpression of this protein could *per se* act as stressor, perhaps favoring oxidative stress, unfolded protein response (UPR), or DNA damage. To assess this point, we first checked by western blotting the expression of several stress markers. The levels of heat-shock chaperonins HSP90 and HSP60, whose up-regulation is induced by oxidative stress, and that of chaperone GRP78/Bip, that binds to nascent polypeptides and participates to the UPR [57], were all found unvaried between 3XF-Iso3 and 3XF-Mock control cells; similarly, no XBP1 spliced form was observed in both cell lines in physiological

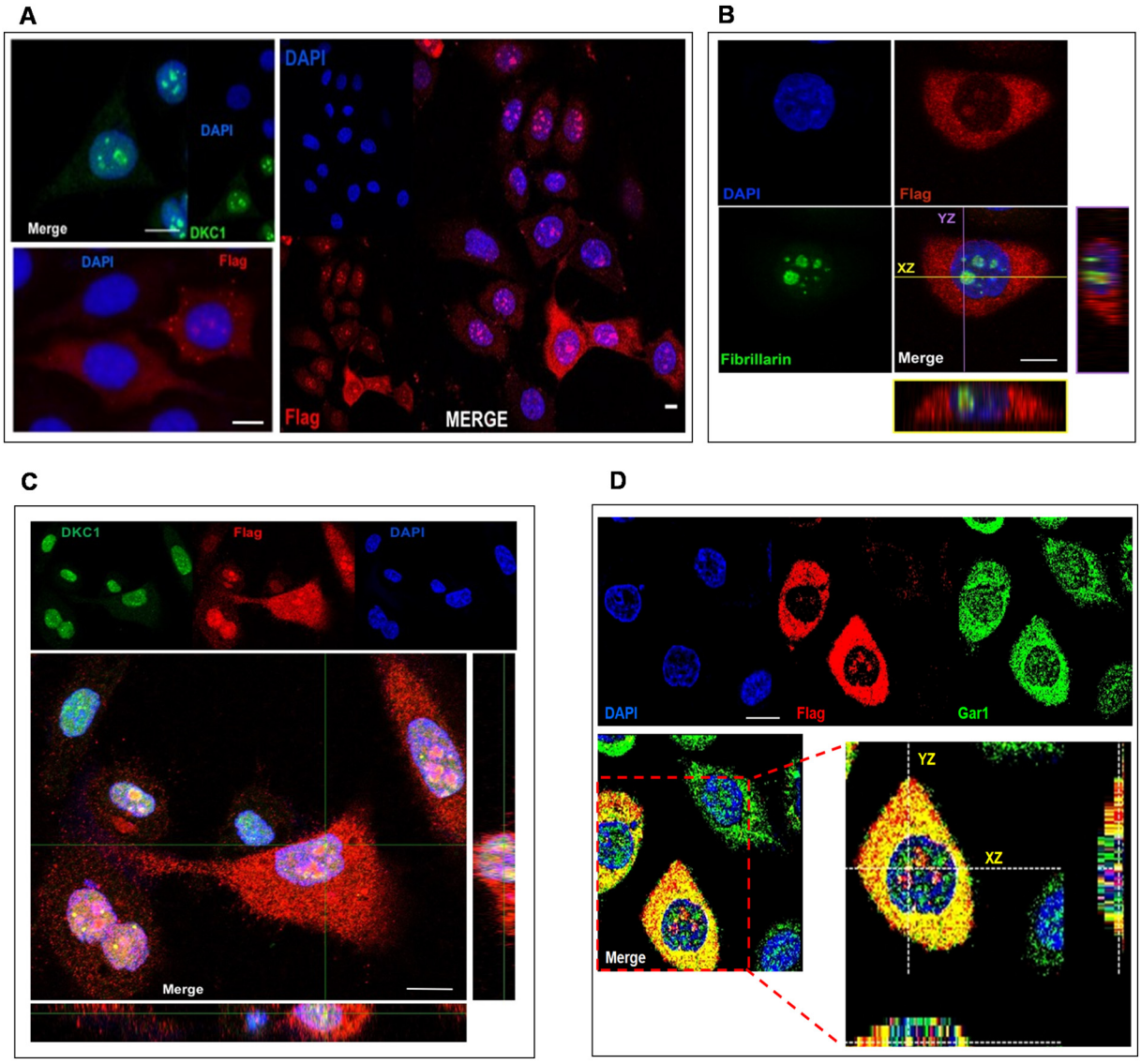

Fig. 1. Dyskerin Iso3 can enter the nucleus, concentrating in the nucleoli and the CBs. (A) Confocal microscopy pictures showing dyskerin Isoform 1 (top left, green) and Isoform 3 (bottom left and right; red) variegated intracellular distribution. IF analysis was performed at least 3 times and extended to different fields of the same microscope slide. Within the nucleus, Iso3 (red) colocalizes with (B) fibrillarin (green) and (C) dyskerin Isoform 1 (green); note that in some HPL cells Isoform 1 is displaced from the internal nucleolar dense fibrillar component. (D) Iso3 (red) colocalizes with Gar1 (green) in cytoplasm and in the nucleus, mainly at the CBs and the nucleolar periphery. 3XF-Iso3 cells were used in all pictures. Nuclei were counterstained with DAPI (blue). Scale Bars: 10 μm.

conditions (Fig. 3A; Appendix A, Supplemental Fig. S3A). In addition, in 3XF-Iso3 cells the c-Jun N-terminal kinase (JNK) and the eIF2α stress-responsive pathways were activated only upon arsenite treatment, as in the 3XF-Mock control (Fig. 3B), confirming that Iso3 overexpression *per se* does not act as stressor. Finally, to check whether the increase in ROS level previously observed in 3XF-Iso3 cells [45] could augment DNA damage, we followed by IF the levels of γH2AX histone variant, whose nuclear foci mark the sites of unrepaired Double Strand Breaks (DSBs). Although γH2AX levels showed high *cell-to-cell variability* in both 3XF-Iso3 cells and control cells (Fig. 3C,D), no positive correlation was observed between the intensity of γH2AX nuclear staining and the level of Iso3 expression (HLP *versus* LLP cells, used as internal control; Fig. 3C), implying that high levels of Iso3 expression did not induce genomic instability. The finding that γH2AX was properly induced in 3XF-Iso3 cells upon exposure to etoposide (Appendix A, Supplemental Fig. S3B), that produces DSBs, indicated that the γH2AX-drived DNA damage response was not impaired in these cells. Collectively, these data indicated that Iso3 overexpression *per se* does not induce cellular stress and confirmed that 3XF-Iso3 cells cope successfully with increased ROS production, having acquired an adaptive response [45].

3.4. Dyskerin Iso3 is dynamically recruited to cytoplasmic RNP granules

Within the cytoplasm, Iso3 shows a punctuate and diffuse pattern (Fig. 1A; Fig. 4A); however, upon arsenite treatment, the protein concentrates into cytoplasmic granules of different sizes, being larger in HLP than in LLP cells (Fig. 4B). This pattern is very similar to that observed in cells overexpressing the G3BP1 SG-nucleating factor, where the protein induces SGs of different sizes in a dose-dependent manner, with higher concentration correlating with larger size of granules [58]. Considering that SG composition is variable, in order to check whether Iso3-positive granules readily corresponded to SGs we stained 3XF-Iso3 cells with several SG markers before (Appendix A, Supplemental Fig. S4) or after arsenite treatment (Fig. 4C–G). In stressed cells, positive correlation was found with TIA1 (Fig. 4C), PABP (Fig. 4D,E), eIF3 (Fig. 4F) and YB1 (Fig. 4G), confirming that Flag-stained aggregates corresponded to *bona fide* SGs. Strikingly, Flag signal also marked some

small granules that remained unstained by SG markers (see Fig. 4E, arrows), suggesting that Iso3 aggregation can precede their coalescence into larger foci. Note that, in our experimental conditions, fibrillarin and nucleophosmin (NPM1/B23), two abundant nucleolar proteins (see Appendix A, Supplemental Fig. S5), were not detected into SGs after arsenite treatment (Fig. 5A,B), further underlining the specificity of Iso3 enrollment in these foci. SGs can be induced by various types of stresses, with their composition varying in dependence of the specific stressor [59]. Considering that dyskerin and Iso3 have both recently been related to OXPHOS metabolism [45,60], we treated cells with malonate, a mitochondrial respiratory chain inhibitor that also induces SGs [61]. Although this compound is a weak SG-inducer [61], Iso3 recruitment was observed also after this treatment (Appendix A, Fig. S6), indicating that diverse stressor types can trigger its aggregation. Composition of SGs is dynamic, with many components shuttling from these granules to P-bodies or GW182 bodies, and *viceversa* [12]. We thus immunostained 3XF-Iso3 cells for the detection of DCP1, a known marker of P-bodies, and of GW182. In absence of stress, we observed only occasional overlap between Flag-stained foci and DCP1 or GW182 bodies (Fig. 6A,B); however, in both cases the colocalization increased upon arsenite treatment (Fig. 6C,D). In this last condition, many Flag-stained foci strictly flank P- and GW182-bodies, consistent with the notion that these foci can physically associate with SGs, often exchanging some components [12]. Hence, depending on stress conditions, Iso3 can transiently and dynamically be recruited to diverse types of cytoplasmic granules.

3.5. H/ACA snoRNP core components can be recruited in SGs

Next, we checked whether endogenous H/ACA snoRNP components might also be recruited in SGs. Localization of canonical full-length dyskerin isoform is generally considered to be restricted to the nucleus, although sporadic reports hinted at additional cytoplasmic localizations [62,63]. Intriguingly, recent Mass Spectrometric analyses (MS) included dyskerin in the SG proteome [4,64], while independent reports showed that this protein interacts with YB1 [65] and G3BP1 [66]. Thus, we attempted to assess dyskerin participation in SGs by IF analyses. Considering that the high concentration of dyskerin in the nucleus could prevent its detection in the cytoplasm, and therefore its identification into SGs, we analyzed confocal images of arsenite-treated cells under overexposure conditions. Under these settings, dyskerin was found to aggregate in small cytoplasmic puncta (Fig. 7 B); in several cells, these puncta were found to coalesce in larger cytoplasmic foci (Fig. 7C) that were co-stained by the canonical PABP marker (Fig. 7D). Hence, also the canonical dyskerin isoform can participate in cytoplasmic SGs. We then asked whether other core components of H/ACA snoRNPs could similarly be enrolled in SG composition. Strikingly, upon arsenite treatment, Gar1 colocalized with Iso3 not only in the nucleus, but also at Iso3-positive cytoplasmic granules (Fig. 8A). The highly efficient Gar1participation in SGs fits well with the protein structural properties since, similarly to G3BP1, Gar1 contains glycine-arginine-rich domains (GAR/RGG disordered motifs [67]) that are known to favor SG assembly by inducing LLPS [64]. Nop10 was instead found to participate poorly in SG formation (Fig. 8B), while Nhp2 formed small puncta and was efficiently engaged into large Iso3-positive granules only in a subset of cells that always corresponded to HLPs (Fig. 8C), thus suggesting that high-level Iso3 expression could promote Nhp2 enrollment in SGs. This scenario hinted at a close relationship between these two proteins and in fact IF and western blotting analyses both showed that Iso3 expression levels correlated with Nhp2 upregulation (Fig. 8D,E).

In conclusion, these results collectively revealed that components of

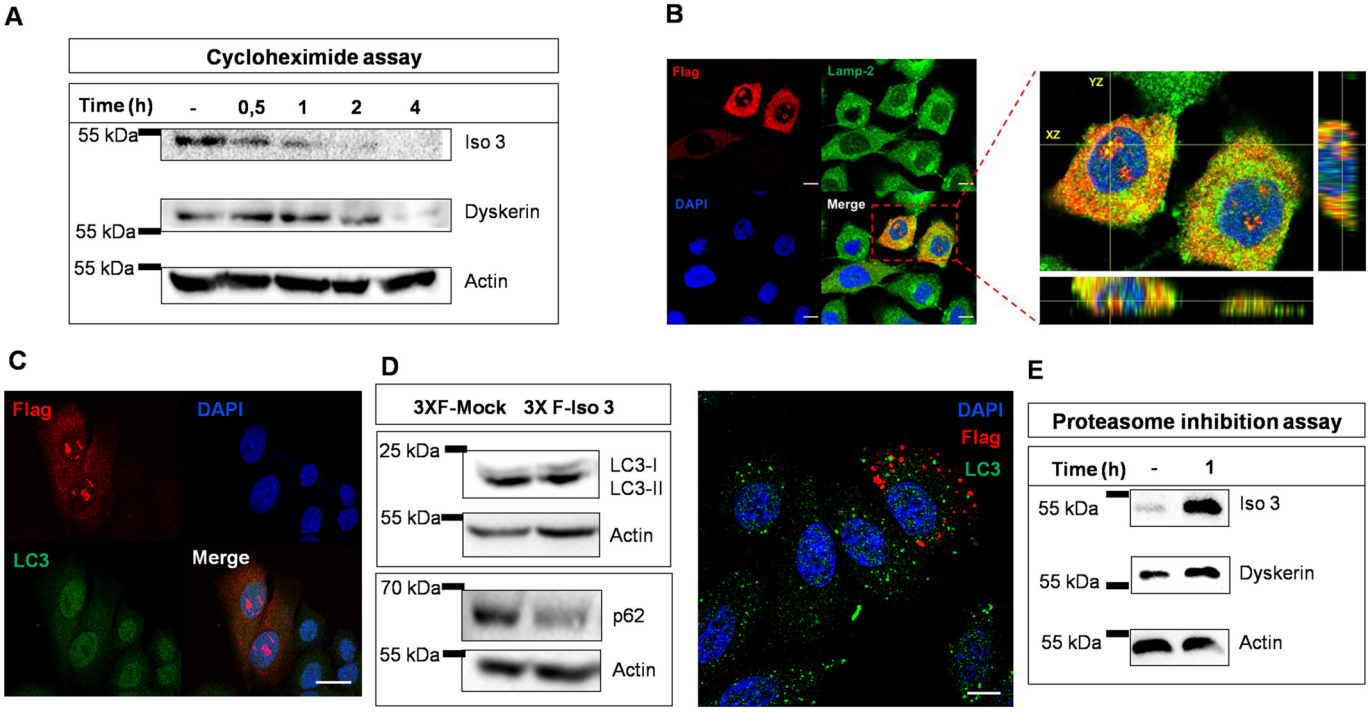

Fig. 2. Variable expression and decay of dyskerin Iso3. (A) Western blot analysis showing the rapid decrease in Iso3 protein level following cycloheximide treatment. The blot is representative of biological triplicates normalized with respect to α-actin (additional replicates are shown in Supplemental Fig. S2A). (B) Confocal microscopy image showing Lamp-2 (green) and Iso3(red) localization; note their partial overlap in the nuclei of HPL cells. (C) Confocal image showing LC3 (green) and Iso3 (red) expression in unstressed cells. (D) Western blot analysis comparing LC3 and p62 expression in 3XF-Iso3 arsenite-treated cells (left) and confocal microscopy image of arsenite-treated cells (right); Iso3 (red), LC3 (green). Note that arsenite treatment triggers Iso3 aggregation in cytoplasmic foci. (E) Proteasome inhibition assay showing a marked and rapid increase of Iso3 accumulation level, indicative of proteasomal-dependent degradation. The blot is representative of biological triplicates normalized with respect to α-actin (additional replicates are shown in Supplemental Fig. S2B). IF analysis was performed at least 3 times and extended to different fields of the same microscope slide. 3XF-Iso3 cells were used in all pictures; nuclei were counterstained with DAPI (blue). Scale Bars: 10 μm.

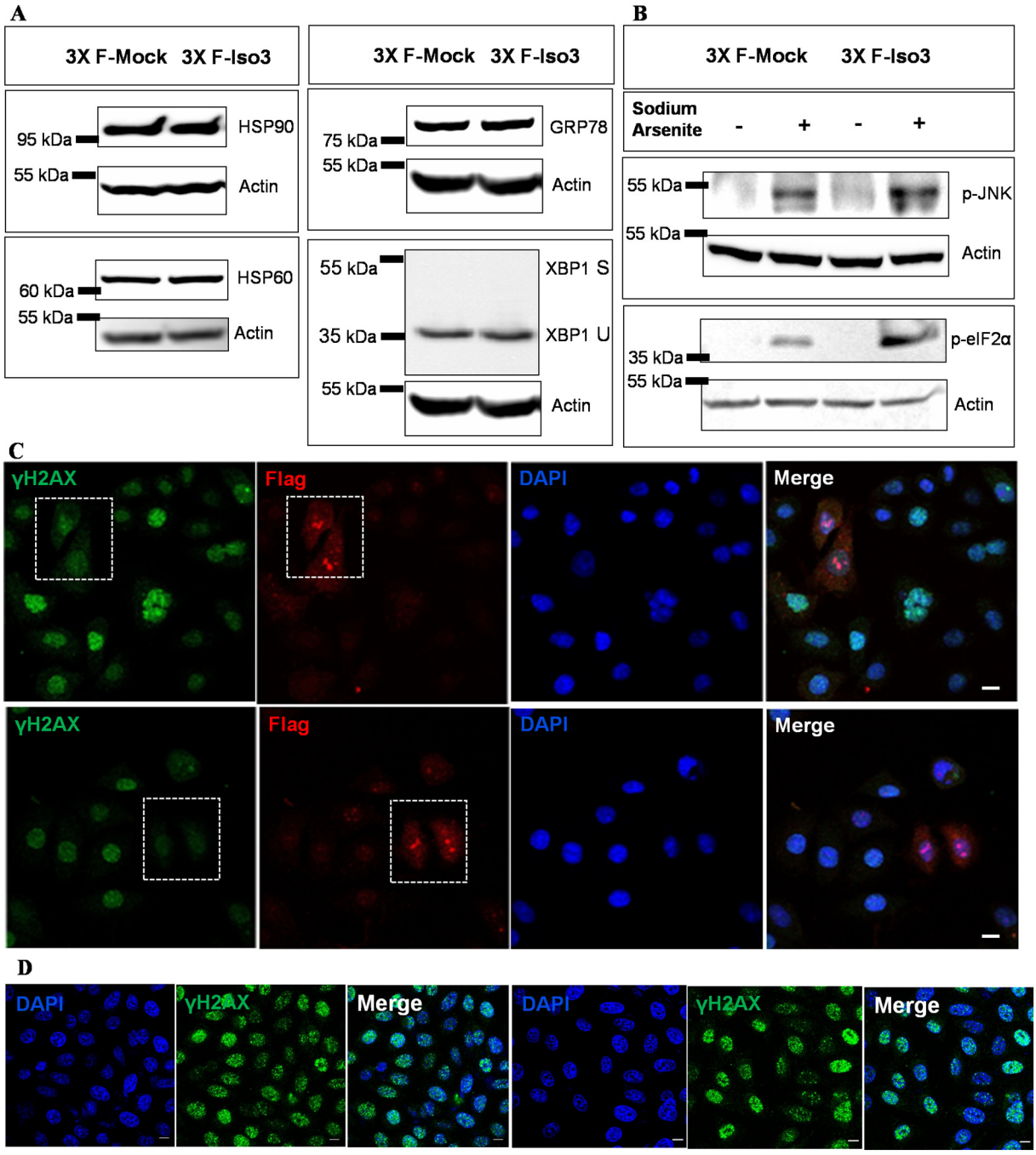

Fig. 3. Dyskerin Iso3 overexpression does not induce oxidative stress, unfolded protein response or DNA damage. (A) Western blot analysis comparing HSP90, HSP60 and GRP78 expression in 3XF-Mock and 3XF-Iso3 unstressed cells. Densitometric quantification of data derived from biological triplicates, normalized with respect to α-actin, is reported in Supplemental Fig. S3A. In absence of stress, the XBP1 spliced form is not induced in both cell lines. (B) Western blot analysis showing that p-JNK and p-eIF2α stress-responsive pathways were induced in both 3XF-Mock and3XF-Iso3 cells only upon arsenite treatment. Confocal immunofluorescence analyses of 3XF-Iso3 (C) and 3XF-Mock cells (D). In (C), note the lack of positive correlation between the intensity of the γH2AX nuclear staining (green) and the level of Iso3 protein expression (red). The dotted squares enclose HPL cells. IF analysis was performed at least 3 times and extended to different fields of the same microscope slide. Nuclei were counterstained with DAPI (blue). Scale Bars: 10 μm.

H/ACA snoRNPs can interact with each-other outside of the nucleus and, through their participation into SGs, can actively contribute in the stress response.

4. Discussion

To gain further insights on the biological functions of the Iso3 dyskerin variant, here we used immunofluorescence microscopy as a sensor of its biological activity. The finding that the expression level of this protein is highly variable and tightly controlled by proteasome-mediated degradation is well consistent with the notion that low-abundance variant isoforms may have more specialized functions, playing significant roles in changing cell status or in modulating cellular physiology. Considering that the dyskerin C-terminal tract is particularly rich in phosphorylation sites, its deletion in the Iso3 variant can furnish a significant distinctive trait, perhaps allowing a different post-translational regulation during the cell cycle or in response to growth conditions. Since recent reports connected Iso3 with either lipid

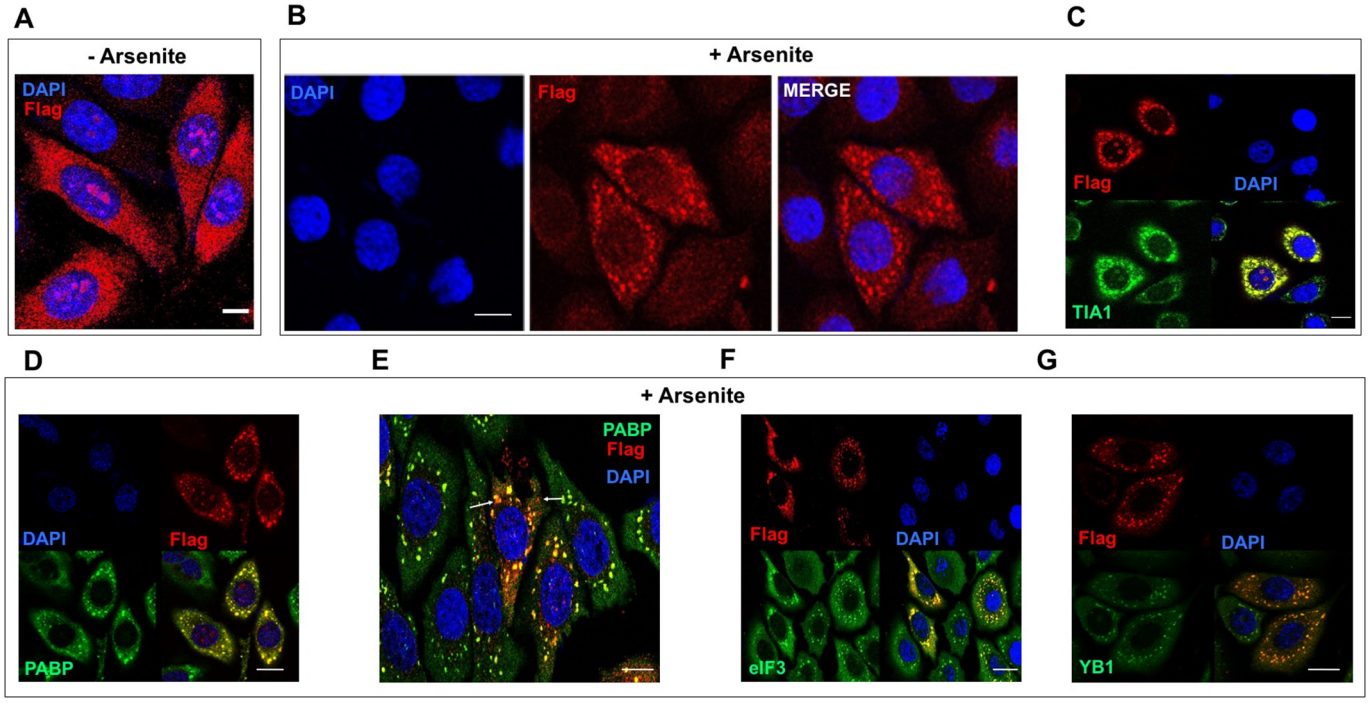

Fig. 4. Dyskerin Iso3 is dynamically recruited to cytoplasmic stress granules. (A) Confocal image showing Iso3 (red) expression in 3XF-Iso3 untreated cells. (B) Upon arsenite treatment, Iso3 is recruited in cytoplasmic granules. (C) In these granules, Iso3 (red) colocalizes with TIA1 (green). (D) Iso3-positive foci (red) are stained also by PABP (green), although, as showed in (E), some of them remain unlabelled by this protein (see arrows). (F) Iso3 foci (red) are marked also by eIF3 (green) and, as showed in (G), by YB1 (green). Intracellular distribution of each protein was checked in at least 3 experiments and the analysis extended to different fields of the same microscope slide. Nuclei were counterstained with DAPI (blue). Scale Bars: 10 μm.

[44] and redox metabolism [45], the possibility that metabolic conditions could be involved in its regulation appears favorable. The dual nucleo-cytoplasmic localization exhibited by this dyskerin isoform represents a further distinctive feature and suggests a possible role in the transduction of intra-cellular signals. Indeed, it is reasonable to suppose that Iso3 might act as nuclear-export chaperone for ribosomal particles, and/or possibly influence translation by contacting ribosomes or cytoplasmic mRNAs, as we previously suggested [43]. This view is in

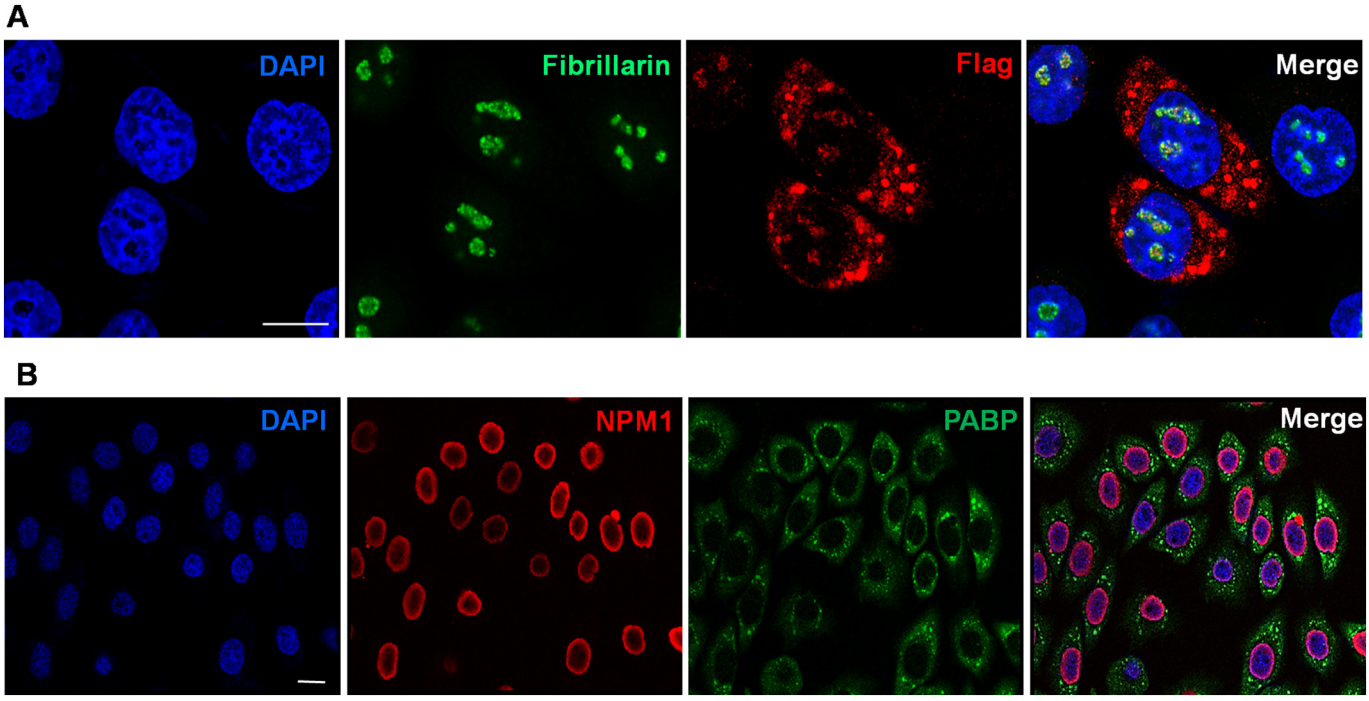

Fig. 5. Specificity of dyskerin Iso3 enrollment in stress granules. (A) Confocal image of arsenite-treated 3XF-Iso3 cells. Note that Iso3 (red) is efficiently engaged in SGs, while the nucleolar protein fibrillarin (green) remains restricted to the nucleus. (B) Upon arsenite treatment, NPM1 (red) relocates at the nuclear periphery, but it is not recruited in PABP-marked (green) SGs. Nuclei were counterstained with DAPI (blue). Scale Bars: 10 μm. Intracellular distribution of each protein was checked in at least 3 experiments and the analysis extended to different fields of the same microscope slide.

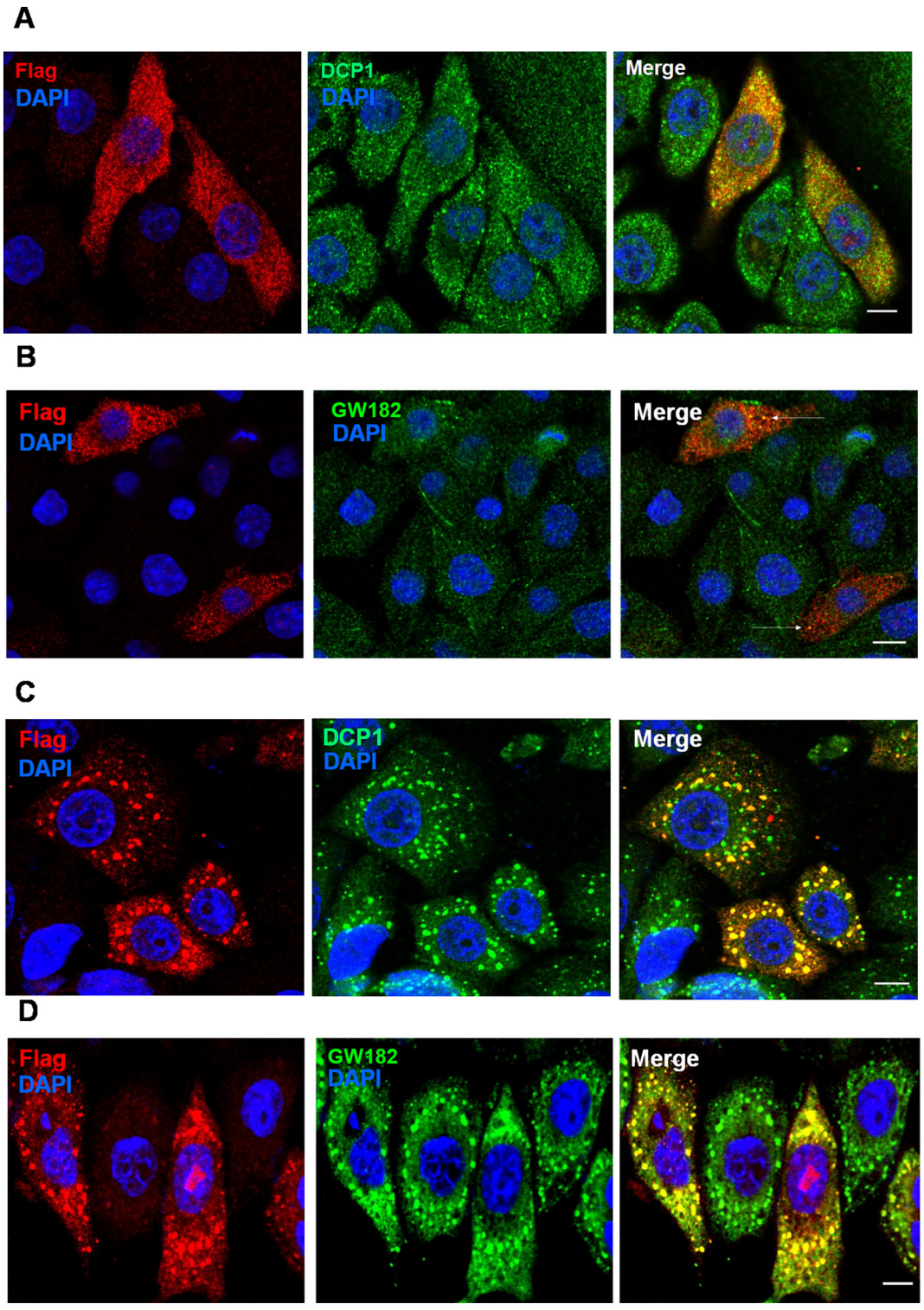

Fig. 6. Promiscuous recruitment of dyskerin Iso3 in cytoplasmic RNP granules. (A) Confocal image of 3XF-Iso3 unstressed cells showing localization of Iso3 (red) and DCP1 (green); in (B), cells were stained for Iso3 (red) and GW182 (green). In absence of stress, only occasional localization was observed in both cases. (C-D) Upon arsenite treatment, Iso3 (red) colocalization with DCP1 (green) or GW182 (green) significantly increased. Intracellular distribution of each protein was checked in at least 3 experiments and the analysis extended to different fields of the same microscope slide. Scale Bars: 10 μm.

keeping with a bulk of recent data indicating that composition, and perhaps activity, of ribosomes may be differently adapted to diverse cell types, or cell status, allowing "specialization" of these organelles [68–70]. Since Iso3 keeps the dyskerin PUA-RNA binding domain, it might also represent a good candidate for the nuclear export of H/ACA snoRNAs. These molecules are in fact currently known to have additional extra-nuclear localization, being detectable even in extracellular fluids [71,72]. Worth noting, snoRNAs are attracting growing interest, being implicated in diverse biological and pathological processes [73], including resistance to lipotoxic stress [74].

The other components of the H/ACA snoRNP tetramer -Nhp2, Nop10 and Gar1-, although generally overlooked, also have a dual

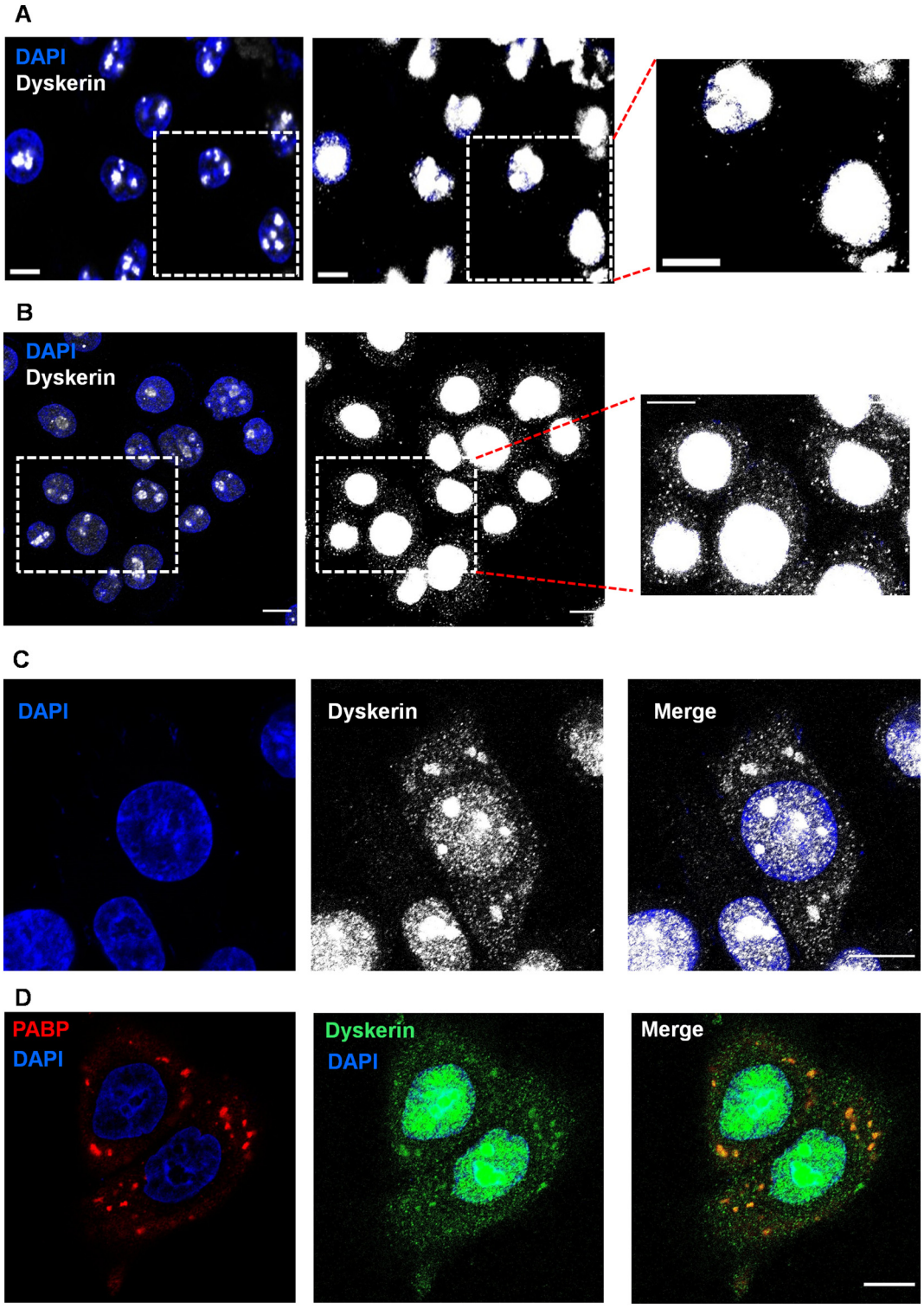

Fig. 7. Dyskerin Isoform 1 forms cytoplasmic puncta in response to stress. (A) Confocal immunofluorescence picture showing localization of dyskerin isoform 1 (gray) in 3XF-Iso3 untreated cells under nucleolar optimal exposure setting; in the middle, the same field where the dyskerin signal was acquired at overexposure conditions; the dotted square is enlarged in the right inset.,(B) Arsenite-treated 3XF-Iso3 cells under nucleolar optimal exposure setting; in the middle the same field where the dyskerin signal was acquired at overexposure conditions revealed that the protein exhibits a cytoplasmic granular pattern. The dotted square is enlarged in the right inset. (C) In HLP cells, dyskerin-positive puncta (gray) can coalesce in larger cytoplasmic granules in which (D) dyskerin (green) colocalizes with PABP (red). Confocal analysis was performed at least 3 times and extended to different fields of the same microscope slide. Nuclei were counterstained with DAPI (blue). Scale Bars: 10 μm.

nucleo-cytoplasmic localization, supporting the possibility that they can play additional extra-nuclear functions, either independently or interacting each-other. Nucleoli and CBs, the nuclear bodies where snoRNPs concentrate, are membrane-less organelles thought to have a liquid droplet-like behavior [7], so their constituents can be in constant influx and out-flux. Resident molecules can be relocated in response to

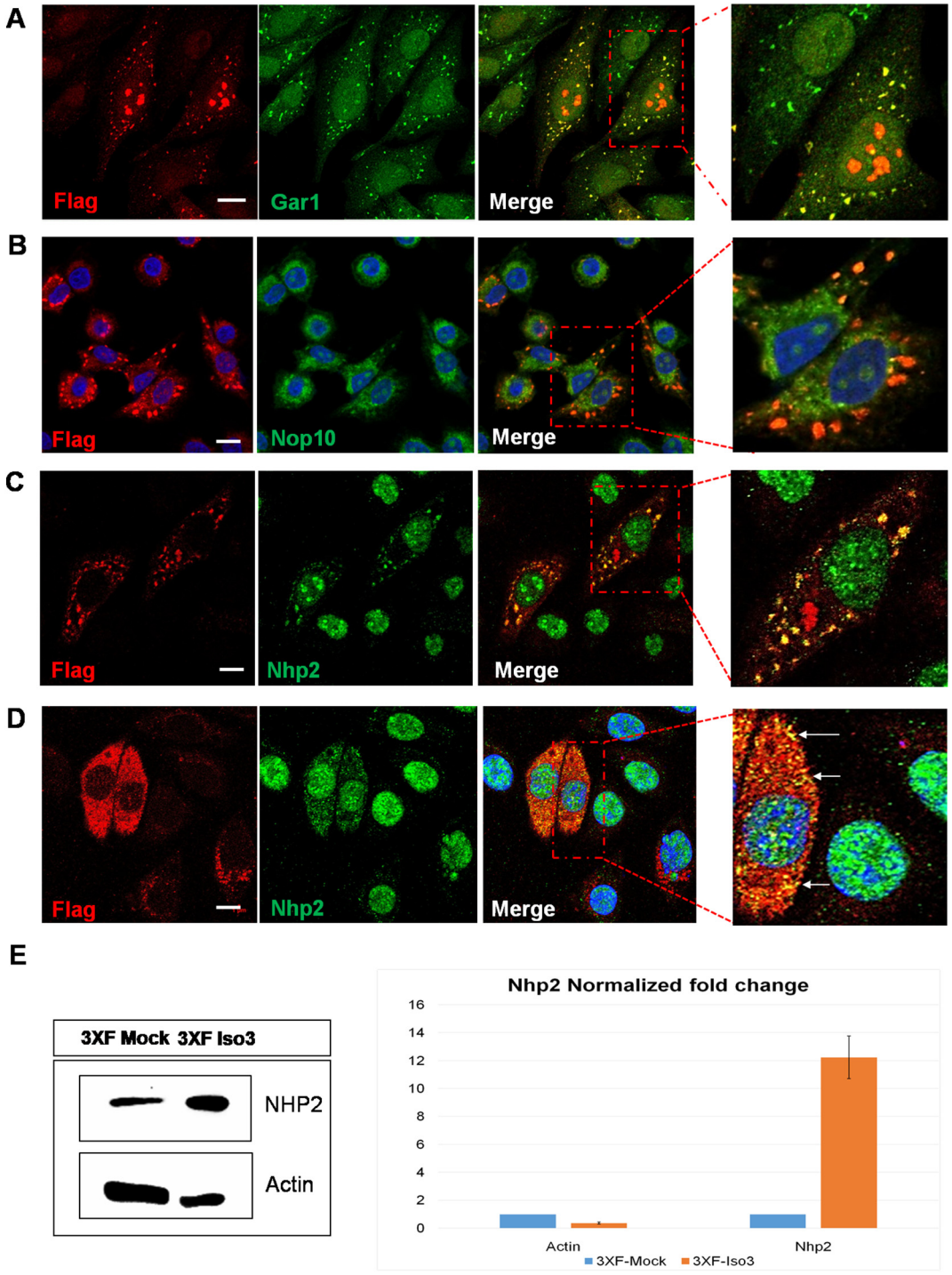

Fig. 8. Core components of H/ACA snoRNPs can be enrolled in SGs. Confocal immunofluorescence pictures of arsenite-treated 3XF-Iso3 cells stained in: (A) for Iso 3 (red) and Gar1 (green); (B) for Iso 3 (red) and Nop10 (green); (C) for Iso3 (red) and Nhp2 (green). Note that Gar1 is efficiently recruited in SGs in all cells, Nop10 is barely recruited, while some Nhp2 is efficiently recruited in large granules only in HLP cells. (D) Immunofluorescence analysis showing correlation between Iso3 expression level with Nhp2 upregulation. Note that in unstressed HLP cells, sporadic Iso3-Nhp2 cytoplasmic colocalization can be observed (see arrows). This correlation was confirmed by (E) western blot and quantitative relative densitometric analysis. In each picture, red dotted squares were enlarged in the right insets. Intracellular distribution of each protein was checked in at least 3 experiments and the analysis extended to different fields of the same microscope slide. Nuclei were counterstained with DAPI (blue). Scale Bars: 10 μm.

environmental, metabolic or stress stimuli, and play different functions in dependence of their specific location in the cell. For example, within the nucleus Iso3 concentrates in the nucleoli and the CBs, a pattern fully coherent with its participation in H/ACA snoRNPs; nonetheless, its capture in these nuclear bodies might have the additional role of down-regulating its further cytoplasmic functions. To this regard, the Iso3 expression pattern turned out to be poorly informative, since outside the nucleus the protein does not concentrate in any specific compartment. However, the finding that it is recruited into SGs shed some light on this issue, and further supports the conclusion that this isoform is involved in the stress response, as suggested by its pro-survival effect [45]. Being SGs also critical redox regulators [75], it is possible that

participation in their assembly might contribute to the ROS tolerance displayed by 3XF-Iso3 cells [45]. Given the Iso3 recruitment in granules unstained by SG markers and its promiscuous transit in P/GW182 bodies, we cannot exclude that this protein can also participate in the "oxidized RNA bodies" identified in HeLa cells exposed to the same stressor [76]. We also showed that SG components generally share common properties, such as containing RNA-binding and IDR regions, and often display a dynamic nucleolar localization [18]; in addition, when overexpressed, they can form cytoplasmic aggregate in a dose-dependent manner even in absence of stress [58]. As showed here, Iso3 displays all these features, including that of forming cytoplasmic foci in unstressed cells. Remarkably, endogenous full-length dyskerin, although generally considered be strictly localized in the nucleus, can also participate in SG assembly. We would underline that the structure of this protein, that contains a RNA-binding domain and IDRs, predicts that it can promote promiscuous interactions with different partners [18,77]. In keeping with this view, at least 198 putative interactors are currently annotated in the dyskerin interactome (available at https://thebiogrid.org), supporting the view that it can participate to multiple, perhaps transient, complexes. Indeed, while dyskerin nuclear localization has well been established, its localization in other cellular compartments did not receive the same grade of investigation. We surmise that the massive concentration of this protein in the nucleoli and the CBs has so far hampered a direct visualization of its trafficking at low-level in the cytoplasm. To this regard, overexpression of the Iso3-Flag-tagged protein can be of invaluable help in facilitating the discovery of new interactions, possibly unmasking new unforeseen roles.

We also reported that at least two other H/ACA snoRNP components, Gar1 and Nhp2, can be efficiently relocated into SGs. Not surprising, Gar1 carries typical GAR/RGG domains and is upregulated in response to DNA-damaging agents [28], raising the possibility that it can take a major role in SG assembly, perhaps promoting aggregation of other snoRNP components through protein-protein interaction. Considering that several diseases can disturb SGs formation or persistence [18,78] the fact that Gar1 dysregulation has been associated not only to dyskeratosis congenita, but also with spinal muscular atrophy [79], is fully consistent with this view. Conversely, the finding that Nop10 has barely been recruited suggests that, at least in the cytoplasm, this component might not coordinately interact with the others during the stress response. Indeed, Nop10 expression correlates poorly with that of other snoRNP proteins. For example, by examining several independent human gene expression profile datasets, Lin et al. [28] observed that Nop10 expression showed no correlation with those of Gar1, Nhp2 and dyskerin, that were instead all well interrelated. Similarly, Von Stedingk et al. [41], based on gene expression profiling, identified a coordinated snoRNP signature for poor prognosis of neuroblastoma patients that included Gar1, Nhp2 and dyskerin, but not Nop10. Thus, it is possible that components of the H/ACA snoRNP tetramer can have additional functions independently from each other, playing uncanonical roles that certainly deserve further investigation. In addition, it cannot be excluded that assembly of these snoRNP components may follow a different pathway, perhaps in the cytoplasm or in stress conditions.

5. Conclusions

By analyzing in detail the dynamic intracellular expression profile of a dyskerin splice variant we observed that H/ACA snoRNPs components, despite being strongly concentrated in the nucleoli and the CBs, can be recruited in SGs. In this way, these proteins can participate in stress response, possibly in concert with other SG components showing a similarly dual nucleo-cytoplasmic localization. These findings revealed for the first time that H/ACA snoRNP components can have additional non-nuclear functions, with their activities possibly depending on the specific sub-cellular localization; furthermore, they imply that H/ACA snoRNPs have a role not only in ribosome biogenesis and rRNA modification, but could also participate in the SG-mediated translational control. These results highlight the deep involvement of these complexes in the regulation of cell homeostasis and further expand the dynamic connection between nucleolar proteins and stress response.

Supplementary data to this article can be found online at https://doi.org/10.1016/j.bbamcr.2019.118529.

Declaration of competing interest

The authors declare no conflict of interest.

Acknowledgments

The authors are grateful to Dr. Rosario Vicidomini for helpful comments and advice on immunofluorescence confocal microscopy analyses and to Dr. Nunzia Di Maio and Dr. Marianna Varone per collaborative organization and support.

Funding

This work was supported by the University Federico II of Naples and by P.O.R. Movie FESR 2007/2013, CUP B25C13000240007 to M.F.

References

[1] A. Lavut, D. Raveh, Sequestration of highly expressed mRNAs in cytoplasmic granules, P-bodies, and stress granules enhances cell viability, PLoS Genet. 8 (2012) e1002527, , https://doi.org/10.1371/journal.pgen.1002527.
[2] P. Anderson, N. Kedersha, Stress granules, Curr. Biol. 19 (2009) R397–R398, https://doi.org/10.1016/j.cub.2009.03.013.
[3] J.R. Buchan, R. Parker, Eukaryotic stress granules: the ins and outs of translation, Mol. Cell 36 (2009) 932–941, https://doi.org/10.1016/j.molcel.2009.11.020.
[4] S. Jain, J.R. Wheeler, R.W. Walters, A. Agrawal, A. Barsic, R. Parker, ATPase-modulated stress granules contain a diverse proteome and substructure, Cell 164 (2016) 487–498, https://doi.org/10.1016/j.cell.2015.12.038.
[5] J.R. Wheeler, T. Matheny, S. Jain, R. Abrisch, R. Parker, Distinct Stages in Stress Granule Assembly and Disassembly, Elife, 5, (2016), https://doi.org/10.7554/eLife.18413.
[6] S. Alberti, Phase separation in biology, Curr. Biol. 27 (2017) R1097–R1102, https://doi.org/10.1016/j.cub.2017.08.069.
[7] A. Nemeth, I. Grummt, Dynamic regulation of nucleolar architecture, CurrOpin Cell Biol 52 (2018) 105–111, https://doi.org/10.1016/j.ceb.2018.02.013.
[8] A.L. Darling, Y. Liu, C.J. Oldfield, V.N. Uversky, Intrinsically disordered proteome of human membrane-less organelles, Proteomics 18 (2018) e1700193, , https://doi.org/10.1002/pmic.201700193.
[9] D.S.W. Protter, B.S. Rao, B. Van Treeck, Y. Lin, L. Mizoue, M.K. Rosen, R. Parker, Intrinsically disordered regions can contribute promiscuous interactions to RNP granule assembly, Cell Rep. 22 (2018) 1401–1412, https://doi.org/10.1016/j.celrep.2018.01.036.
[10] J.R. Buchan, mRNP granules, Assembly, function, and connections with disease, RNA Biol 11 (2014) 1019–1030, https://doi.org/10.4161/15476286.2014.972208.
[11] Z. Yang, A. Jakymiw, M.R. Wood, T. Eystathioy, R.L. Rubin, M.J. Fritzler, E.K. Chan, GW182 is critical for the stability of GW bodies expressed during the cell cycle and cell proliferation, J. Cell Sci. 117 (2004) 5567–5578, https://doi.org/10.1242/jcs.01477.
[12] G. Stoecklin, N. Kedersha, Relationship of GW/P-bodies with stress granules, Adv. Exp. Med. Biol. 768 (2013) 197–211, https://doi.org/10.1007/978-1-4614-5107-5_12.
[13] N. Kedersha, G. Stoecklin, M. Ayodele, P. Yacono, J. Lykke-Andersen, M.J. Fritzler, D. Scheuner, R.J. Kaufman, D.E. Golan, P. Anderson, Stress granules and processing bodies are dynamically linked sites of mRNP remodeling, J. Cell Biol. 169 (2005) 871–884, https://doi.org/10.1083/jcb.200502088.
[14] X. Wang, L. Chang, H. Wang, A. Su, Z. Wu, Dcp1a and GW182 induce distinct cellular aggregates and have different effects on microRNA pathway, DNA Cell Biol. 36 (2017) 565–570, https://doi.org/10.1089/dna.2017.3633.
[15] N.P. Hoyle, L.M. Castelli, S.G. Campbell, L.E. Holmes, M.P. Ashe, Stress-dependent relocalization of translationally primed mRNPs to cytoplasmic granules that are kinetically and spatially distinct from P-bodies, J. Cell Biol. 179 (2007) 65–74, https://doi.org/10.1083/jcb.200707010.
[16] C. von Roretz, S. Di Marco, R. Mazroui, I.E. Gallouzi, Turnover of AU-rich-containing mRNAs during stress: a matter of survival, Wiley Interdiscip Rev RNA 2 (2011) 336–347, https://doi.org/10.1002/wrna.55.
[17] M. Hofweber, D. Dormann, Friend or foe - post-translational modifications as regulators of phase separation and RNP granule dynamics, J Biol Chem (2018), https://doi.org/10.1074/jbc.TM118.001189.
[18] H. Mahboubi, U. Stochaj, Nucleoli and stress granules: connecting distant relatives, Traffic 15 (2014) 1179–1193, https://doi.org/10.1111/tra.12191.

[19] A. Angrisani, R. Vicidomini, M. Turano, M. Furia, Human dyskerin: beyond telomeres, Biol. Chem. 395 (2014) 593–610, https://doi.org/10.1515/hsz-2013-0287.
[20] A. Henras, Y. Henry, C. Bousquet-Antonelli, J. Noaillac-Depeyre, J.P. Gelugne, M. Caizergues-Ferrer, Nhp2p and Nop10p are essential for the function of H/ACA snoRNPs, EMBO J. 17 (1998) 7078–7090, https://doi.org/10.1093/emboj/17.23.7078.
[21] D.L. Lafontaine, D. Tollervey, Birth of the snoRNPs: the evolution of the modification-guide snoRNAs, Trends Biochem. Sci. 23 (1998) 383–388.
[22] U.T. Meier, RNA modification in Cajal bodies, RNA Biol. 14 (2017) 693–700, https://doi.org/10.1080/15476286.2016.1249091.
[23] S.B. Cohen, M.E. Graham, G.O. Lovrecz, N. Bache, P.J. Robinson, R.R. Reddel, Protein composition of catalytically active human telomerase from immortal cells, Science 315 (2007) 1850–1853, https://doi.org/10.1126/science.1138596.
[24] M. Penzo, L. Rocchi, S. Brugiere, D. Carnicelli, C. Onofrillo, Y. Couté, M. Brigotti, L. Montanaro, Human ribosomes from cells with reduced dyskerin levels are intrinsically altered in translation, FASEB J. 29 (2015) 3472–34.82, https://doi.org/10.1096/fj.15-270991.
[25] B.W. Gu, M. Bessler, P.J. Mason, A pathogenic dyskerin mutation impairs proliferation and activates a DNA damage response independent of telomere length in mice, Proc. Natl. Acad. Sci. U. S. A. 105 (2008) 10173–10178, https://doi.org/10.1073/pnas.0803559105.
[26] B.W. Gu, J.M. Fan, M. Bessler, P.J. Mason, Accelerated hematopoietic stem cell aging in a mouse model of dyskeratosis congenita responds to antioxidant treatment, Aging Cell 10 (2011) 338–348, https://doi.org/10.1111/j.1474-9726.2011.00674.x.
[27] L. Pereboeva, E. Westin, T. Patel, I. Flaniken, L. Lamb, A. Klingelhutz, F. Goldman, DNA damage responses and oxidative stress in dyskeratosis congenita, PLoS One 8 (2013) e76473, , https://doi.org/10.1371/journal.pone.0076473.
[28] P. Lin, M.E. Mobasher, Y. Hakakian, V. Kakarla, A.F. Naseem, H. Ziai, F. Alawi, Differential requirements for H/ACA ribonucleoprotein components in cell proliferation and response to DNA damage, Histochem. Cell Biol. 144 (2015) 543–558, https://doi.org/10.1007/s00418-015-1359-6.
[29] G. Tortoriello, J.F. de Celis, M. Furia, Linking pseudouridine synthases to growth, development and cell competition, FEBS J. 277 (2010) 3249–3263, https://doi.org/10.1111/j.1742-4658.2010.07731.x.
[30] R. Vicidomini, A. Di Giovanni, A. Petrizzo, L.F. Iannucci, G. Benvenuto, A.C. Nagel, A. Preiss, M. Furia, Loss of Drosophila pseudouridine synthase triggers apoptosis-induced proliferation and promotes cell-nonautonomous EMT, Cell Death Dis. 6 (2015) e1705, , https://doi.org/10.1038/cddis.2015.68.
[31] R. Vicidomini, A. Petrizzo, A. di Giovanni, L. Cassese, A.A. Lombardi, C. Pragliola, M. Furia, Drosophila dyskerin is required for somatic stem cell homeostasis, Sci. Rep. 7 (2017) 347, https://doi.org/10.1038/s41598-017-00446-8.
[32] N.S. Heiss, S.W. Knight, T.J. Vulliamy, S.M. Klauck, S. Wiemann, P.J. Mason, A. Poustka, I. Dokal, X-linked dyskeratosis congenita is caused by mutations in a highly conserved gene with putative nucleolar functions, Nat. Genet. 19 (1998) 32–38, https://doi.org/10.1038/ng0598-32.
[33] S.W. Knight, N.S. Heiss, T.J. Vulliamy, C.M. Aalfs, C. McMahon, P. Richmond, A. Jones, R.C. Hennekam, A. Poustka, P.J. Mason, I. Dokal, Unexplained aplastic anaemia, immunodeficiency, and cerebellar hypoplasia (Hoyeraal-Hreidarsson syndrome) due to mutations in the dyskeratosis congenita gene, DKC1, Br. J. Haematol. 107 (1999) 335–339.
[34] M.E. Schaner, D.T. Ross, G. Ciaravino, T. Sorlie, O. Troyanskaya, M. Diehn, Y.C. Wang, G.E. Duran, T.L. Sikic, S. Caldeira, H. Skomedal, I.P. Tu, T. Hernandez-Boussard, S.W. Johnson, P.J. O'Dwyer, M.J. Fero, G.B. Kristensen, A.L. Borresen-Dale, T. Hastie, R. Tibshirani, M. van de Rijn, N.N. Teng, T.A. Longacre, D. Botstein, P.O. Brown, B.I. Sikic, Gene expression patterns in ovarian carcinomas, Mol. Biol. Cell 14 (2003) 4376–4386, https://doi.org/10.1091/mbc.e03-05-0279.
[35] S.L. McDonald, H.D. Edington, J.M. Kirkwood, D. Becker, Expression analysis of genes identified by molecular profiling of VGP melanomas and MGP melanoma-positive lymph nodes, Cancer Biol Ther 3 (2004) 110–120.
[36] F. Westermann, K.O. Henrich, J.S. Wei, W. Lutz, M. Fischer, R. Konig, R. Wiedemeyer, V. Ehemann, B. Brors, K. Ernestus, I. Leuschner, A. Benner, J. Khan, M. Schwab, High Skp2 expression characterizes high-risk neuroblastomas independent of MYCN status, Clin. Cancer Res. 13 (2007) 4695–4703, https://doi.org/10.1158/1078-0432.CCR-06-2818.
[37] M. Turano, A. Angrisani, M. De Rosa, P. Izzo, M. Furia, Real-time PCR quantification of human DKC1 expression in colorectal cancer, Acta Oncol. 47 (2008) 1598–1599, https://doi.org/10.1080/02841860801898616.
[38] P. Sieron, C. Hader, J. Hatina, R. Engers, A. Wlazlinski, M. Muller, W.A. Schulz, DKC1 overexpression associated with prostate cancer progression, Br. J. Cancer 101 (2009) 1410–1416, https://doi.org/10.1038/sj.bjc.6605299.
[39] A. Witkowska, J. Gumprecht, J. Glogowska-Ligus, G. Wystrychowski, A. Owczarek, M. Stachowicz, A. Bocianowska, E. Nowakowska-Zajdel, U. Mazurek, Expression profile of significant immortalization genes in colon cancer, Int. J. Mol. Med. 25 (2010) 321–329.
[40] B. Liu, J. Zhang, C. Huang, H. Liu, Dyskerin overexpression in human hepatocellular carcinoma is associated with advanced clinical stage and poor patient prognosis, PLoS One 7 (2012) e43147, , https://doi.org/10.1371/journal.pone.0043147.
[41] K. von Stedingk, J. Koster, M. Piqueras, R. Noguera, S. Navarro, S. Pahlman, R. Versteeg, I. Ora, D. Gisselsson, D. Lindgren, H. Axelson, snoRNPs regulate telomerase activity in neuroblastoma and are associated with poor prognosis, Transl. Oncol. 6 (2013) 447–457.
[42] M. Penzo, V. Ludovini, D. Treré, A. Siggillino, J. Vannucci, G. Bellezza, L. Crinò L, L. Montanaro, Dyskerin and TERC expression may condition survival in lung cancer patients, Oncotarget, 6 (2015) 21755–21760.
[43] A. Angrisani, M. Turano, L. Paparo, C. Di Mauro, M. Furia, A new human dyskerin isoform with cytoplasmic localization, BiochimBiophys Acta 1810 (2011) 1361–1368, https://doi.org/10.1016/j.bbagen.2011.07.012.
[44] N. Thyagarajan, J.D. Marshall, A.T. Pickett, C. Schumacher, Y. Yang, S.L. Christian, R.J. Brown, Transcriptomic analysis of THP-1 macrophages exposed to lipoprotein hydrolysis products generated by lipoprotein lipase, Lipids 52 (2017) 189–205, https://doi.org/10.1007/s11745-017-4238-1.
[45] A. Angrisani, N. Matrone, V. Belli, R. Vicidomini, N. Di Maio, M. Turano, F. Scialo, P.A. Netti, A. Porcellini, M. Furia, A functional connection betweendyskerin and energy metabolism, Redox Biol. 14 (2018) 557–565, https://doi.org/10.1016/j.redox.2017.11.003.
[46] J. He, B.W. Gu, J. Ge, Y. Mochizuki, M. Bessler, P.J. Mason, Variable expression of Dkc1 mutations in mice, Genesis 47 (2009) 366–373, https://doi.org/10.1002/dvg.20509.
[47] I. Fernandez-Garcia, T. Marcos, A. Munoz-Barrutia, D. Serrano, R. Pio, L.M. Montuenga, C. Ortiz-de-Solorzano, Multiscale in situ analysis of the role of dyskerin in lung cancer cells, Integr Biol (Camb) 5 (2013) 402–413, https://doi.org/10.1039/c2ib20219k.
[48] X. Darzacq, N. Kittur, S. Roy, Y. Shav-Tal, R.H. Singer, U.T. Meier, Stepwise RNP assembly at the site of H/ACA RNA transcription in human cells, J. Cell Biol. 173 (2006) 207–218, https://doi.org/10.1083/jcb.200601105.
[49] S. Schwartz, D.A. Bernstein, M.R. Mumbach, M. Jovanovic, R.H. Herbst, B.X. Leon-Ricardo, J.M. Engreitz, M. Guttman, R. Satija, E.S. Lander, G. Fink, A. Regev, Transcriptome-wide mapping reveals widespread dynamic-regulated pseudouridylation of ncRNA and mRNA, Cell 159 (2014) 148–162, https://doi.org/10.1016/j.cell.2014.08.028.
[50] T.M. Carlile, M.F. Rojas-Duran, B. Zinshteyn, H. Shin, K.M. Bartoli, W.V. Gilbert, Pseudouridine profiling reveals regulated mRNA pseudouridylation in yeast and human cells, Nature 515 (2014) 143–146, https://doi.org/10.1038/nature13802.
[51] J. Karijolich, C. Yi, Y.T. Yu, Transcriptome-wide dynamics of RNA pseudouridylation, Nat Rev Mol Cell Biol 16 (2015) 581–585, https://doi.org/10.1038/nrm4040.
[52] M.E. Brault, C. Lauzon, C. Autexier, Dyskeratosis congenita mutations in dyskerin SUMOylation consensus sites lead to impaired telomerase RNA accumulation and telomere defects, Hum. Mol. Genet. 22 (2013) 3498–3507, https://doi.org/10.1093/hmg/ddt204.
[53] N. Mizushima, Autophagy: process and function, Genes Dev. 21 (2007) 2861–2873, https://doi.org/10.1101/gad.1599207.
[54] K.R. Drake, M. Kang, A.K. Kenworthy, Nucleocytoplasmic distribution and dynamics of the autophagosome marker EGFP-LC3, PLoS One 5 (2010) e9806, , https://doi.org/10.1371/journal.pone.0009806.
[55] N.L. Kedersha, M. Gupta, W. Li, I. Miller, P. Anderson, RNA-binding proteins TIA-1 and TIAR link the phosphorylation of eIF-2 alpha to the assembly of mammalian stress granules, J. Cell Biol. 147 (1999) 1431–1442.
[56] G. Bjorkoy, T. Lamark, S. Pankiv, A. Overvatn, A. Brech, T. Johansen, Monitoring autophagic degradation of p62/SQSTM1, Methods Enzymol. 452 (2009) 181–197, https://doi.org/10.1016/S0076-6879(08)03612-4.
[57] K.F.R. Pobre, G.J. Poet, L.M. Hendershot, The endoplasmic reticulum (ER) chaperone BiP is a master regulator of ER functions: getting by with a little help from ERdj friends, J. Biol. Chem. (2018), https://doi.org/10.1074/jbc.REV118.002804.
[58] L.C. Reineke, J.D. Dougherty, P. Pierre, R.E. Lloyd, Large G3BP-induced granules trigger eIF2alpha phosphorylation, Mol. Biol. Cell 23 (2012) 3499–3510, https://doi.org/10.1091/mbc.E12-05-0385.
[59] A. Aulas, M.M. Fay, S.M. Lyons, C.A. Achorn, N. Kedersha, P. Anderson, P. Ivanov, Stress-specific differences in assembly and composition of stress granules and related foci, J. Cell Sci. 130 (2017) 927–937, https://doi.org/10.1242/jcs.199240.
[60] J.S. Ibanez-Cabellos, G. Perez-Machado, M. Seco-Cervera, E. Berenguer-Pascual, J.L. Garcia-Gimenez, F.V. Pallardo, Acute telomerase components depletion triggers oxidative stress as an early event previous to telomeric shortening, Redox Biol. 14 (2018) 398–408, https://doi.org/10.1016/j.redox.2017.10.004.
[61] X. Fu, X. Gao, L. Ge, X. Cui, C. Su, W. Yang, X. Sun, W. Zhang, Z. Yao, X. Yang, J. Yang, Malonate induces the assembly of cytoplasmic stress granules, FEBS Lett. 590 (2016) 22–33, https://doi.org/10.1002/1873-3468.12049.
[62] S. Orru, A. Aspesi, M. Armiraglio, M. Caterino, F. Loreni, M. Ruoppolo, C. Santoro, I. Dianzani, Analysis of the ribosomalprotein S19 interactome, Mol. Cell. Proteomics 6 (2007) 382–393, https://doi.org/10.1074/mcp.M600156-MCP200.
[63] H.M. Koskimaa, K. Kurvinen, S. Costa, K. Syrjanen, S. Syrjanen, Molecular markers implicating early malignant events in cervical carcinogenesis, Cancer Epidemiol. Biomark. Prev. 19 (2010) 2003–2012, https://doi.org/10.1158/1055-9965.EPI-09-0781.
[64] S. Boeynaems, E. Bogaert, D. Kovacs, A. Konijnenberg, E. Timmerman, A. Volkov, M. Guharoy, M. De Decker, T. Jaspers, V.H. Ryan, A.M. Janke, P. Baatsen, T. Vercruysse, R.M. Kolaitis, D. Daelemans, J.P. Taylor, N. Kedersha, P. Anderson, F. Impens, F. Sobott, J. Schymkowitz, F. Rousseau, N.L. Fawzi, W. Robberecht, P. Van Damme, P. Tompa, L. Van Den Bosch, Phase Separation of C9orf72 Dipeptide Repeats Perturbs Stress Granule Dynamics, Mol. Cell 65 (2017) 1044–1055, https://doi.org/10.1016/j.molcel.2017.02.013 e1045.
[65] J.R. Hutchins, Y. Toyoda, B. Hegemann, I. Poser, J.K. Heriche, M.M. Sykora, M. Augsburg, O. Hudecz, B.A. Buschhorn, J. Bulkescher, C. Conrad, D. Comartin, A. Schleiffer, M. Sarov, A. Pozniakovsky, M.M. Slabicki, S. Schloissnig, I. Steinmacher, M. Leuschner, A. Ssykor, S. Lawo, L. Pelletier, H. Stark, K. Nasmyth, J. Ellenberg, R. Durbin, F. Buchholz, K. Mechtler, A.A. Hyman, J.M. Peters, Systematic analysis of human protein complexes identifies chromosome segregation proteins, Science 328 (2010) 593–599, https://doi.org/10.1126/science.1181348.
[66] E.L. Huttlin, R.J. Bruckner, J.A. Paulo, J.R. Cannon, L. Ting, K. Baltier, G. Colby, F. Gebreab, M.P. Gygi, H. Parzen, J. Szpyt, S. Tam, G. Zarraga, L. Pontano-Vaites, S. Swarup, A.E. White, D.K. Schweppe, R. Rad, B.K. Erickson, R.A. Obar, K.G. Guruharsha, K. Li, S. Artavanis-Tsakonas, S.P. Gygi, J.W. Harper, Architecture

of the human interactome defines protein communities and disease networks, Nature 545 (2017) 505–509, https://doi.org/10.1038/nature22366.
[67] P. Thandapani, T.R. O'Connor, T.L. Bailey, S. Richard, Defining the RGG/RG motif, Mol. Cell 50 (2013) 613–623, https://doi.org/10.1016/j.molcel.2013.05.021.
[68] N.R. Genuth, M. Barna, The discovery of ribosome heterogeneity and its implications for gene regulation and organismal life, Mol. Cell 71 (2018) 364–374, https://doi.org/10.1016/j.molcel.2018.07.018.
[69] P. Calamita, G. Gatti, A. Miluzio, A. Scagliola, S. Biffo, Translating the game: ribosomes as active players, Front. Genet. 9 (2018) 533, https://doi.org/10.3389/fgene.2018.00533.
[70] M. Penzo, L. Montanaro, Turning uridines around: role of rRNA Pseudouridylation in ribosome biogenesis and ribosomal function, Biomolecules 8 (2018) E38, , https://doi.org/10.3390/biom8020038.
[71] J.E. Freedman, M. Gerstein, E. Mick, J. Rozowsky, D. Levy, R. Kitchen, S. Das, R. Shah, K. Danielson, L. Beaulieu, F.C. Navarro, Y. Wang, T.R. Galeev, A. Holman, R.Y. Kwong, V. Murthy, S.E. Tanriverdi, M. Koupenova, E. Mikhalev, K. Tanriverdi, Corrigendum: diverse human extracellular RNAs are widely detected in human plasma, Nat. Commun. 7 (2016) 11902, https://doi.org/10.1038/ncomms11902.
[72] S.U. Umu, H. Langseth, C. Bucher-Johannessen, B. Fromm, A. Keller, E. Meese, M. Lauritzen, M. Leithaug, R. Lyle, T.B. Rounge, A comprehensive profile of circulating RNAs in human serum, RNA Biol. 15 (2018) 242–250, https://doi.org/10.1080/15476286.2017.1403003.
[73] T. Cao, S. Rajasingh, S. Samanta, B. Dawn, D.C. Bittel, J. Rajasingh, Biology and clinical relevance of noncoding sno/scaRNAs, Trends Cardiovasc Med 28 (2018) 81–90, https://doi.org/10.1016/j.tcm.2017.08.002.
[74] O.A. Youssef, S.A. Safran, T. Nakamura, D.A. Nix, G.S. Hotamisligil, B.L. Bass, Potential role for snoRNAs in PKR activation during metabolic stress, Proc. Natl. Acad. Sci. U. S. A. 112 (2015) 5023–5028, https://doi.org/10.1073/pnas.1424044112.
[75] M. Takahashi, M. Higuchi, H. Matsuki, M. Yoshita, T. Ohsawa, M. Oie, M. Fujii, Stress granules inhibit apoptosis by reducing reactive oxygen species production, Mol. Cell. Biol. 33 (2013) 815–829, https://doi.org/10.1128/MCB.00763-12.
[76] Y. Zhan, J.S. Dhaliwal, P. Adjibade, J. Uniacke, R. Mazroui, W. Zerges, Localized control of oxidized RNA, J. Cell Sci. 128 (2015) 4210–4219, https://doi.org/10.1242/jcs.175232.
[77] R.G. Armando, D.L. Mengual Gomez, E.I. Juritz, P. LorenzanoMenna, D.E. Gomez, Homology model and docking-based virtual screening for ligands of human dyskerin as new inhibitors of telomerase for cancer treatment, Int J Mol Sci 19 (2018), https://doi.org/10.3390/ijms19103216.
[78] S. Markmiller, S. Soltanieh, K.L. Server, R. Mak, W. Jin, M.Y. Fang, E.C. Luo, F. Krach, D. Yang, A. Sen, A. Fulzele, J.M. Wozniak, D.J. Gonzalez, M.W. Kankel, F.B. Gao, E.J. Bennett, E. Lecuyer, G.W. Yeo, Context-dependent and disease-specific diversity in protein interactions within stress granules, Cell 172 (2018) 590–604 e513 https://doi.org/10.1016/j.cell.2017.12.032.
[79] L. Pellizzoni, J. Baccon, B. Charroux, G. Dreyfuss, The survival of motor neurons (SMN) protein interacts with the snoRNP proteins fibrillarin and GAR1, Curr. Biol. 11 (2001) 1079–1088.